Lawrence Berkeley National Laboratory
Lawrence Berkeley National Laboratory

### Title
Design and implementation of a vacuum compatible laser-based sub-nm resolution absolute distance measurement gauge

### Permalink
https://escholarship.org/uc/item/9s19s7q0

### Authors
Naulleau, Patrick P.
Denham, Paul E.
Rekawa, Senajith

### Publication Date
2004-02-16

Peer reviewed

eScholarship.org Powered by the California Digital Library
University of California

# Design and implementation of a vacuum compatible laser-based sub-nm resolution absolute distance measurement gauge

Patrick P. Naulleau, Paul E. Denham, and Senajith Rekawa

Center for X-Ray Optics, Lawrence Berkeley National Laboratory, Berkeley, CA 94720

**Abstract**

We describe the design and implementation of a vacuum compatible laser-based absolute distance measurement gauge with sub-nm resolution. The present system is compatible with operation in the $10^{-8}$ Torr range and with some minor modifications could be used in the $10^{-9}$ Torr range. The system is based on glancing incidence reflection and dual segmented diode detection. The system has been implemented as a focus sensor for extreme ultraviolet interferometry and microlithography experiments at Lawrence Berkeley National Laboratory's Advanced Light Source synchrotron radiation facility and 1σ operational measurement noise floor of 0.26 nm has been demonstrated.

**Keyword:** distance measuring, focus sensing, vaccum, synchrotron

## 1. Introduction

Accurate distance sensing is an important capability in many advanced systems such as high-resolution microscopy and lithography. Furthermore, to push the resolution of these systems, the tendency is to reduce the wavelength to regimes where in-vacuum operation is required, complicating the sensor design. Examples of such systems are extreme ultraviolet and soft X-ray microscopy, interferometry, and lithography **[1-6]**. It is also often highly desirable to measure the distance to some target at the same location and time as some other operation is occurring often precluding the use of obscuring sensors such a capacitance sensors. Obvious examples of this would be microscopy and microlithography systems, which require a clear optical path above the target for light propagation.

Here we describe the design and implementation of an absolute distance measurement system compatible with the above requirements. The described system is compatible with operation in the $10^{-8}$ Torr range and with some minor modifications could be used in the $10^{-9}$ Torr range. The laser-based system relies on glancing incidence reflection from the target and dual segmented diode detection of the reflected light. Appropriate optical design of the input and output channels makes the system nominally insensitive to tilt of the target. The described system has been implemented as a focus sensor for extreme ultraviolet interferometry and microlithography experiments at Lawrence Berkeley National Laboratory's Advanced Light Source synchrotron radiation facility. The sensor has been demonstrated to have a 1σ operational measurement noise floor of 0.26 nm.

## 2. Optical design

The optical design of the sensor is a conventional grazing-incidence design with imaging optics in both the input and output channels. Figure 1 shows both a CODE V **[7]** view of a typical optical

layout and a CAD rendering of this same system including fiber-optic source and detector components. The laser illumination is delivered to the sensor through fiber optics with the output illumination from the fiber being re-focus to a pinhole serving as the point source for the sensor. This configuration allows the laser source modules to be placed outside the vacuum chamber. The point source is then re-imaged to the target surface and the light reflected from the surface is again re-imaged to a segmented diode.

Imaging the source to the test piece and re-imaging the same location of the test piece to the segmented diode detector provides for nominal insensitivity to target tilt. This insensitivity to tilt about the image point will strictly hold to the extent that the output channel is corrected for point-to-point imaging. The tilt insensitivity can be explained heuristically by noting that tilting the target can be viewed as synthesizing a larger divergence from the illumination point. In a properly focused, well-corrected lens, this new set of rays will image to the identical point as does the untilted bundle of rays [Fig 2(a)]. Figure 2(b) illustrates the systems optical response to height change of the target. Reflection from the surface causes the re-imaged point source to be displaced in height by a factor of two compared to the surface displacement. This point is then re-imaged to the segmented diode. The displacement at the diode will depend on the magnification chosen for the output branch. In the implementation presented here, the magnification was unity. To add tilt-measurement capabilities to the device, multiple sensor branches may be employed, each imaged to different location on the target.

The implementation presented here utilizes simple spherical singlets for both the input and output branches imaging optics. It is evident that a more sophisticated imaging systems could be employed, however, as described below, we have found this simple low-cost implementation to be more than adequate for nm-scale operations.

The segmented diode used in the implementation presented here is a dual diode, thus the entire measurement range of the distance sensor is limited by the imaged spot size at the diode. The measurement range can be extended somewhat through defocus of the detector, however, this would comes at the cost of increased tilt sensitivity. The capture range could in principle be greatly extended through the use of position-sensitive detectors or linear detector arrays. We note that in practice we have found position sensitive detectors to provide inadequate sensitivity without optical magnification. We have not tested the use of linear arrays. Using the dual-diode method, we have been able to achieve a measurement range of approximately 35 μm. Combined with a resolution of approximately 0.5 nm (two times the noise floor), this translates to a dynamic range of 1 part in 70,000.

## 3. Detection electronics

As described above, the light detector used in our implementation is a dual diode. The position of the beam is determined from the normalized differential detected current. Achieving a target resolution of better than a nm and a measurement range on the order of 35 μm or greater, requires current detection with greater than 16-bit dynamic range above the noise floor. This places great demands on the detector electronics as well as cabling issues related to transferring signals out of the vacuum chamber. To address these issues, a custom vacuum-compatible 20-bit analog-to-digital current converter module has been implemented. The module is based on the Burr-Brown/Texas Instruments DDC112 analog-to-digital converter chip **[8]**. The detector electronics are placed directly into the vacuum chamber allowing the leads from the diodes to the converter to be as short as possible and to remain entirely within the thermally and atmospherically stable vacuum chamber. Onboard digital interface electronics are used to rout the digital signals out of the vacuum chamber to PC-based I/O electronics.

The implementation presented here utilizes 3 sensor branches yielding a total of 6 current signals that must be read. For optimal efficiency and common-mode noise rejection, the converter

module provides for parallel detection of all 6 currents with the values being passed to the control computer in one 120-bit sequence.

**4. Implementation and characterization**

The system described above has been implemented as a wafer height sensor for focus control in an experimental 0.3 numerical aperture (NA) microfield EUV lithography tool being developed at Lawrence Berkeley National Laboratory. Having an operational depth of focus of approximately 100-nm, this lithography tools requires focus control capabilities of 10-nm or better. The implemented system utilizes three separate sensor branches to provide both height and tilt sensitivity. The system uses simple spherical lenses in the input and output branches operating in the unity magnification 4f condition. The focal length for each lens is 63.5 mm. The operational grazing angle to the wafer surface is 3 degrees. Such a small angle was required due to the short (< 5mm) working distance of the 0.3-NA lithographic optic. Figure 3 shows a photograph of the system installed on a calibration and test fixture. The sensor components are mounted to a plate which itself is hard mounted to the optic housing structure. This guarantees stability between the sensor and the optic as is required for meaningful focus control.

The source components were comprised of multimode laser diodes and multimode fibers. Tests showed better overall noise performance with the use of multimode as opposed to single-mode components. This is presumable due to a reduction in speckle contrast, varying speckle across the detector plane would be seen as variations in height.

Figure 4 shows the sensor measurement results from the implemented system operating in vacuum. The operating pressure was approximately $9\times10^{-8}$ Torr. The wafer stage was actuated to generate a series of nominally 19-nm steps in height, which are clearly resolved by the sensor. The apparent jitter at the step edges is believed to be real and attributable to poor damping of the

wafer stage. Another important metric is the long-term stability of the system. Figure 5 shows an overnight plot of the height-sensor readings. We see a large height change (approximately 1 μm) over the first several hours and then the system stabilizes. This height change is real and is attributable to a thermo-electrically cooled CCD camera buried within the wafer stage being turned off at the end of the day. Operating at approximately –35° C, this camera, which is used for interferometric operations [3], has significant thermal effects on surrounding structure. Figure 6 shows a detail of the last few hours from the plot in Fig. 5. Analyzing the performance of the height sensor over this time frame, we find an rms noise floor of 0.26 nm (1.95 nm peak-to-valley). This can be taken as the ultimate resolution limit of the implemented system.

**5. Discussion**

A low-cost vacuum compatible absolute distance measurement gauge with sub-nm resolution has been demonstrated. The described system is compatible with vacuum operation in the $10^{-8}$ Torr range, limited primarily by the fiber optics. Improving the packaging of the fibers, operation could readily be extended to the $10^{-9}$ Torr range. Not relying on any moving parts, the system is robust and stable. Moreover, the non-interferometric nature of this device means that no indexing or fringe counting is required. The system has been tested both on bare and patterned surfaces with no noticeable change in performance. We note that a potential drawback of this system, however, is susceptibility to speckle and non-uniform optical path contamination. Any effect causing morphological changes to the beam at the detector plane will cause distance-reading errors. Speckle can be mitigated through proper selection of source components. Also, long-term changes in beam morphology can, in principle, be corrected through recalibration of the system.

Another limitation of this system is its relatively small working range. The sensor implemented here has been demonstrated to have an operational range of approximately 40 μm and a

linear range of approximately 20 μm. Non-linearity can be corrected through proper calibration, but extending the operational range without effecting resolution is more complicated. As described above, defocus, position sensitive detectors, and linear detector arrays provide options for extended operational range, however, potentially not without sacrifice of resolution. We have observed the resolution trade-off with both the defocus and position sensitive detector approaches. Another option is to add more branches with intentional height offsets and using a bootstrapping approach. This, in principle, would come at the cost of complexity only, not resolution.

This research was performed at Lawrence Berkeley National Laboratory and supported by International Sematech. Lawrence Berkeley National Laboratory is operated under the auspices of the Director, Office of Science, Office of Basic Energy Science, of the US Department of Energy.

## References


1. W. Chao, E. Anderson, G. Denbeaux, B. Harteneck, A. Pearson, D. Olynick, F. Salmassi, C. Song, D. Attwood, "Demonstration of 20 nm half-pitch spatial resolution with soft X-ray microscopy," J. Vac. Sci. & Technol. B **21**, 3108-3111 (2003).
2. A. Pearson, W. Chao, G. Denbeaux, T. Eimueller, P. Fischer, L. Johnson, M. Koehler, C. Larabell, M. Le Gros, D. Yager, D. Attwood, "XM-1: the high-resolution soft X-ray microscope at the Advanced Light Source," Proc. SPIE **Vol. 4146**, 54-59 (2000).
3. K. Goldberg, P. Naulleau, P. Denham, S. Rekawa, K. Jackson, E. Anderson, J. Liddle and J. Bokor, "At-Wavelength Interferometry of the 0.3 NA MET Optic," J. Vac. Sci. & Technol. B **21**, 2706-2710 (2003).
4. P. Naulleau, K. Goldberg, E. Anderson, P. Batson, P. Denham, S. Rekawa, and J, Bokor, "At wavelength characterization of the Engineering Test Stand Set-2 optic," J. Vac. Sci. & Technol. B **19**, 2396-2400 (2001).
5. P. Naulleau, K. Goldberg, E. Anderson, D. Attwood, P. Batson, J. Bokor, P. Denham, E. Gullikson, B. Harteneck, B. Hoef, K. Jackson, D. Olynick, S. Rekawa, F. Salmassi, K. Blaedel, H. Chapman, L. Hale, P. Mirkarimi, R. Soufli, E. Spiller, D. Sweeney, J. Taylor, C. Walton, D. O'Connell, R. Stulen, D. Tichenor, C. Gwyn, P. Yan and G. Zhang, "Sub-70-nm EUV Lithography at the Advanced Light Source Static Microfield Exposure Station Using the ETS Set-2 Optic, " J. Vac. Sci. & Technol. B **20**, 2829-2833 (2002).
6. R. Stulen and D. Sweeney, "Extreme ultraviolet lithography," IEEE J. Quantum Electron. **35**, 694-699 (1999).
7. CODE V is a registered trademark of Optical Research Associates, 3280 E. Foothill Blvd., Pasadena, CA 91107.

8. Technical information on the DDC112 analog-to-digital current converter can be found on the Texas Instruments web site at http://focus.ti.com/docs/prod/folders/print/ddc112.html.

**List of Figures**

Fig. 1. (a) CODE V view of typical optical layout and (b) CAD rendering of system including fiber-optic source components.

Fig. 2. Diagram illustrating optical response to (a) tilt of the target and (b) height change of the target. Angles and distances are greatly exaggerated compared to actual design for illustrative purposes.

Fig. 3. Photograph of implemented wafer height sensor in testing fixtur

Fig. 4. Wafer height sensor measurement results from the implemented system operating in vacuum. The operating pressure was approximately $9\times10^{-8}$ Torr. The wafer stage was actuated to generate a series of nominally 19-nm steps in height. The apparent jitter is believed to be real and attributable to poor damping of the wafer stage

Fig. 5. Overnight plot of the height-sensor readings. A large height change (approximately 1 μm) is seen over the first several hours and then the system stabilizes. This height change is real and is attributable to a thermo-electrically cooled CCD camera buried within the wafer stage being turned off at the end of the day.

Fig. 6. Detail of the last few hours from the plot in Fig. 5. The plot demonstrates an rms noise floor of 0.26 nm (1.95 nm peak-to-valley).

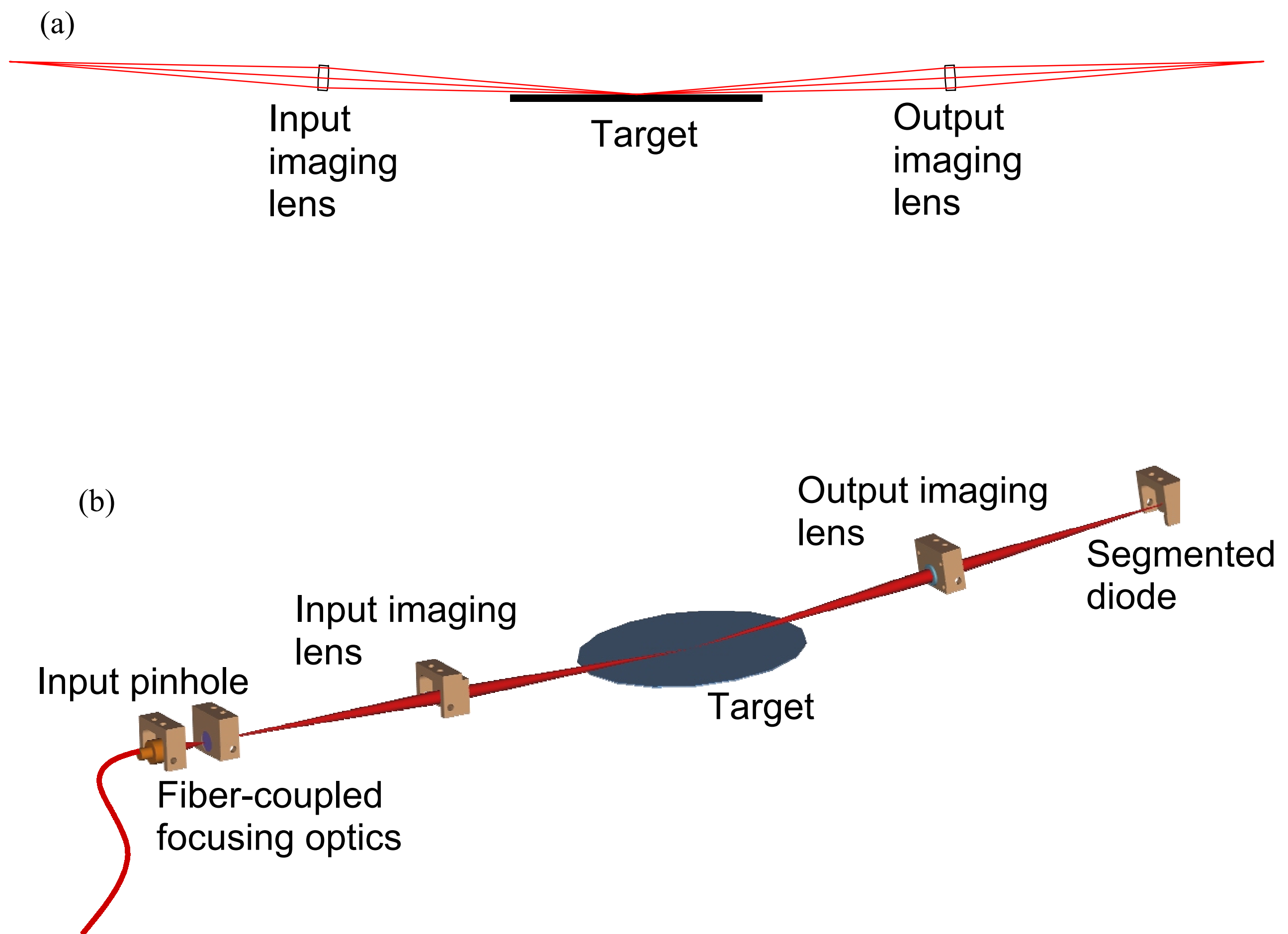


**Fig. 1.** (a) CODE V view of typical optical layout and (b) CAD rendering of system including fiber-optic source components.

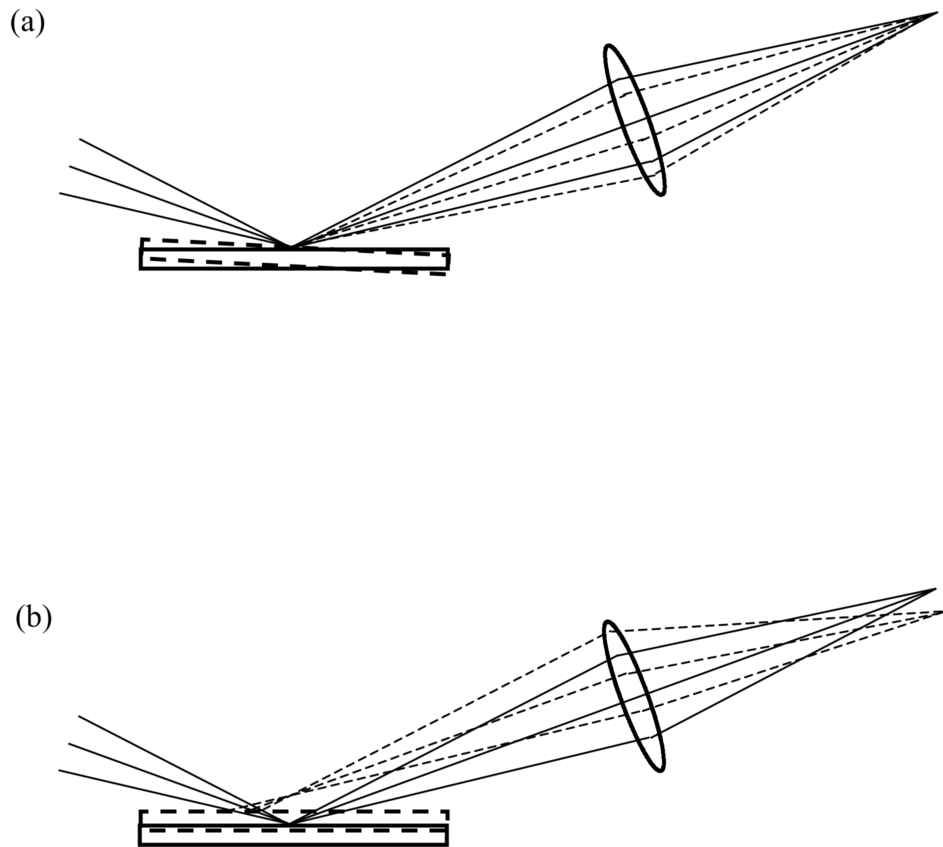


**Fig. 2.** Diagram illustrating optical response to (a) tilt of the target and (b) height change of the target. Angles and distances are greatly exaggerated compared to actual design for illustrative purposes.

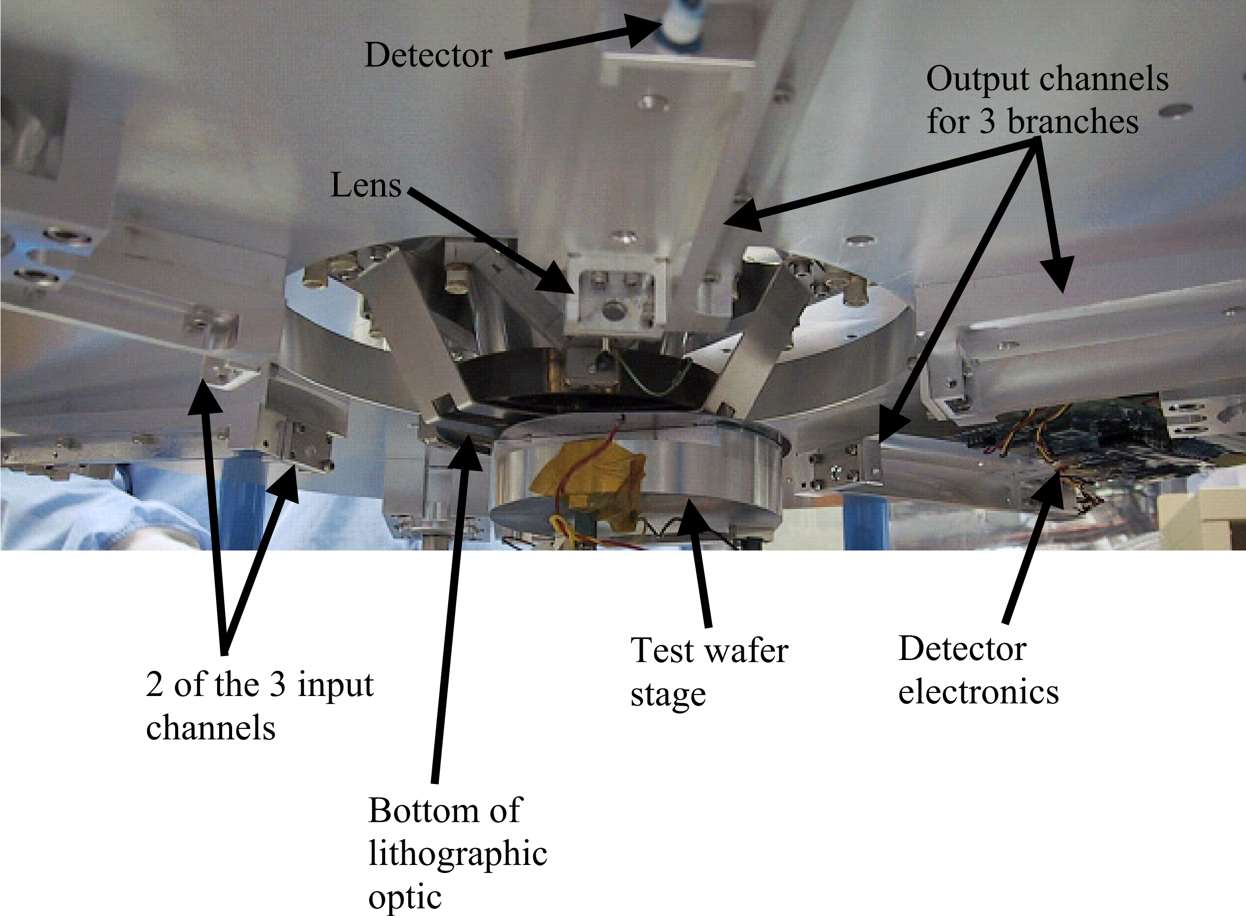


**Fig. 3.** Photograph of implemented wafer height sensor in testing fixture.

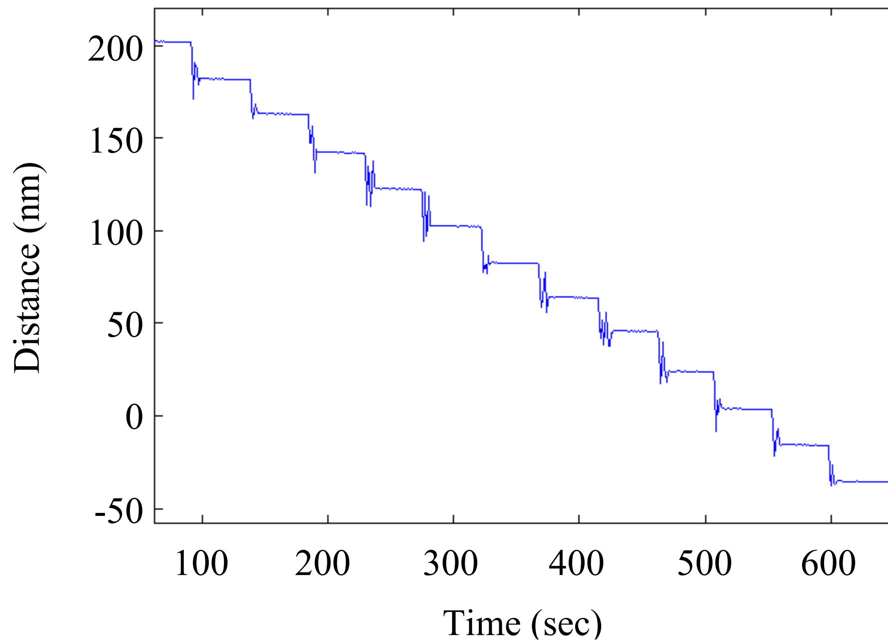


**Fig. 4.** Wafer height sensor measurement results from the implemented system operating in vacuum. The operating pressure was approximately $9\times10^{-8}$ Torr. The wafer stage was actuated to generate a series of nominally 19-nm steps in height. The apparent jitter is believed to be real and attributable to poor damping of the wafer stage.

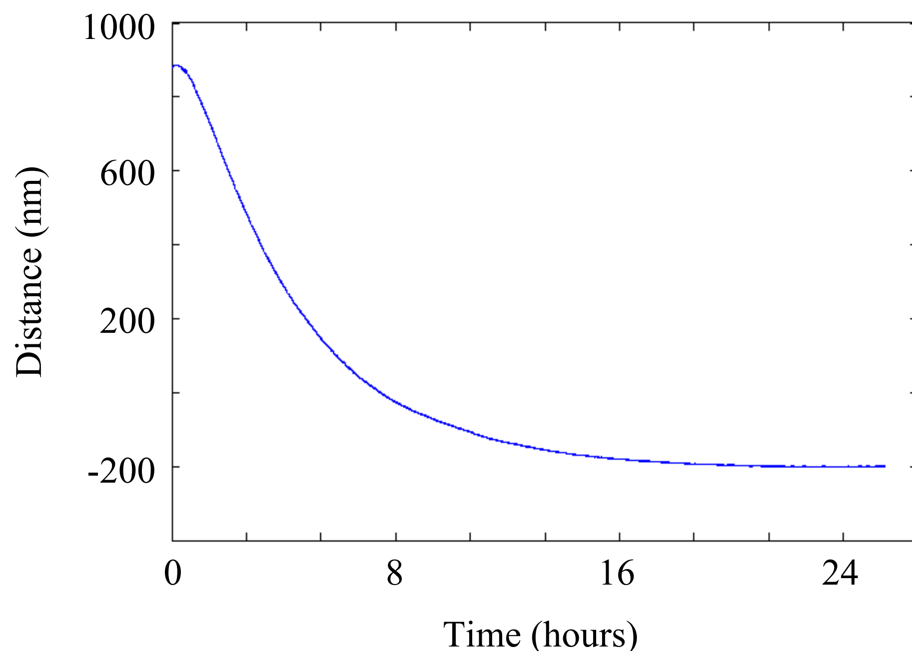


**Fig. 5.** Overnight plot of the height-sensor readings. A large height change (approximately 1 μm) is seen over the first several hours and then the system stabilizes. This height change is real and is attributable to a thermo-electrically cooled CCD camera buried within the wafer stage being turned off at the end of the day.

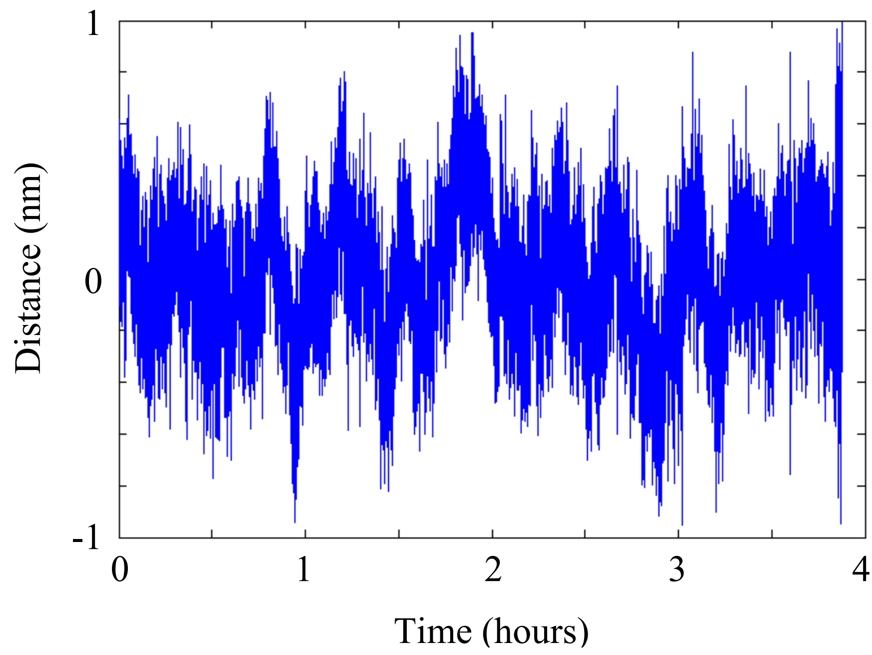


**Fig. 6.** Detail of the last few hours from the plot in Fig. 5. The plot demonstrates an rms noise floor of 0.26 nm (1.95 nm peak-to-valley).